Evaluation of the WOCSS Wind Analysis Scheme for the San Francisco Bay Area

ALISON F. C. BRIDGER, ALLEN J. BECKER, FRANCIS L. LUDWIG,* AND ROY M. ENDLICH*

Department of Meteorology, San Jose State University, San Jose, California

(Manuscript received 26 July 1993, in final form 22 February 1994)

ABSTRACT

Applications of the Winds on Critical Streamline Surfaces (WOCSS) model in the San Francisco Bay Area are described. Three case studies, chosen to represent important classes of airflow in the region, were conducted. Two cases involved a prevailing northwesterly flow with or without an inversion, and the third case involved northeasterly flow at the time of the Oakland hills firestorm of 20 October 1991. The dependence of model results (surface winds) on input winds and on the specification of inversion topography is discussed. Dependable results are produced with relatively few well-placed surface observations and with a single sounding. The results suggest that the model is quite suitable for routine, real-time analyses and other practical applications.

1. Introduction

The Winds on Critical Streamline Surfaces (WOCSS) analysis scheme (Ludwig et al. 1991) was developed to produce high-resolution three-dimensional gridded wind analyses in areas of complex terrain. WOCSS belongs to that class of models that use the principle of mass conservation to compute gridded winds, given as input surface wind observations and wind and temperature soundings, possibly limited in number.

Presumably, the most accurate wind analyses and forecasts on the mesoscale could be obtained from three-dimensional primitive equation models (e.g., Anthes and Warner 1978; those discussed by Pielke 1984). However, the quality of output is strongly dependent on the quality of input data and on the specification of boundary conditions. The fidelity of the results decays as one gets further from the initial conditions. This shortcoming can be addressed by incorporating observations as they become available during the simulation period, but regardless of the correction approaches used, these models require substantial computing resources.

Some success in forecasting and diagnosing mesoscale winds has come from using one-level and one-layer models (e.g., Mass and Dempsey 1985), although in constructing these models simplifying assumptions about the vertical structure of the boundary layer atmosphere are made. While diagnostic models using mass conservation cannot explicitly incorporate important physical processes (such as radiation, nonlinear dynamics, hydrology, etc.), they have the advantage that they execute very quickly on microcomputers (Ludwig et al. 1991). To the degree that they are accurate, these models can therefore be used in the field to produce results quickly. This would be especially important, for example, in the generation of wind data for input to dispersion models in the event of accidental toxic spills or releases. It should be mentioned that mass conservation models can incorporate the effects of some physical processes, such as thermal stratification. Constraints such as these ensure reasonable physical consistency between the model and the atmosphere. Other potential applications include nowcasts for aviation and forest fire management, generation of wind input for forecasting water waves in limited regions, and the placement of meteorological observing platforms.

The WOCSS analysis scheme is described in detail by Ludwig and Endlich (1988). It uses the critical streamline concept (see, e.g., McNider et al. 1984) to restrict vertical motion under stable conditions. The critical streamline concept limits the vertical rise of the flow to that height where the potential energy gained by displacement against a stable thermal stratification equals the kinetic energy of the flow at its original altitude. The WOCSS model also imposes a two-dimensional nondivergence constraint to force flow interaction with the terrain. Very briefly, the defining relationships and steps in the calculation process are as follows:

1) The highest and lowest terrain points in the domain are identified.

2) The user then specifies the heights of flow surfaces above the lowest terrain point, and the model generates a corresponding set of terrain-following surfaces.

* Additional affiliation: SRI International, Menlo Park, California.

Corresponding author address: Dr. Alison F. C. Bridger, Department of Meteorology, San Jose State University, One Washington Square, San Jose, CA 95192-0104.

3) First-guess winds and potential temperature lapse rates are interpolated to these terrain-following surfaces.

4) The interpolated winds and lapse rates over the lowest terrain point are used to determine the highest elevation $(z_{\max})_i$ to which the ith flow surface can rise above the terrain. The expression is

$$(z_{\max})_i = (z_{\min})_i + \frac{V_0}{[g(\partial\theta/\partial z)_0/V_0]^{1/2}}$$

for stable lapse rates,

or

$$(z_{\max})_i = (z_{\min})_i + (\Delta H)_{\max}$$

for neutral or unstable lapse rates.

Here, $(z_{\min})_i$ is the height of the ith surface above the lowest terrain point; $(\Delta H)_{\max}$ is the difference in elevation between the highest and lowest terrain points; $(\partial\theta/\partial z)_0$ is the potential temperature lapse rate and V_0 the wind speed, both on the ith surface above the lowest terrain point; and g is the gravitational acceleration. If the atmosphere were always uniformly stratified, the above relationships would be sufficient to define a set of surfaces that parallel one another, all rising by the same amount over the higher terrain. However, the real atmosphere is frequently characterized by stable layers that have neutral or unstable layers above or below them. Therefore, it is necessary to impose additional constraints on the heights to which the flow is allowed to rise.

5) The maximum elevations for the flow surfaces are constrained such that

$$[(z_{\max})_{i+1} - (z_{\max})_i] \leqslant 0.5[(z_{\min})_{i+1} - (z_{\min})_i]$$

and

$$[(z_{\max})_{i+1} - (z_{\max})_i] \leqslant [(z_{\max})_i - (z_{\max})_{i-1}].$$

The first condition prevents the lower surfaces from penetrating or approaching too closely to higher surfaces, while the second condition keeps terrain influences from penetrating elevated stable layers (and thus prevents the deflection of flow into less stable layers aloft).

6) After the maximum heights to which the air can reach have been defined for each flow surface, that information is used to define the flow surface heights z_i above each grid point. Here it is assumed that the extreme elevations of the critical streamline surfaces are found over the lowest and highest terrain points ($H_{\min}$ and $H_{\max}$, respectively) and that the following proportionality relationship holds over other locations:

$$z_i = (z_{\min})_i + \frac{[H - H_{\min}]}{(\Delta H)_{\max}}[(z_{\max})_i - (z_{\min})_i],$$

where H is the terrain height. It should be noted that the lower flow surfaces often intersect the higher terrain features when there are stable layers present.

7) The observed winds are then interpolated to the newly defined critical streamline flow surfaces. The wind speeds are set to zero wherever a flow surface intersects the terrain.

8) The WOCSS model next iteratively adjusts the flow on each surface toward two-dimensional (within the critical streamline flow surfaces) nondivergence. This forces deflection of the flow by terrain features when conditions are stable.

The iterative approach used to remove divergence will not do so completely in areas where there is strong convergence. This is both a strength and a weakness. It makes the model very stable computationally, but it does not always achieve mass consistency, and it will tend to smooth any regions of strong divergence or convergence. Thus, although this smoothing tends to reduce the influence of unrepresentative data, it also weakens any convergence lines that may exist. As Ludwig et al. (1991) noted, the model should probably include provisions for using the residual divergence to correct vertical motions and obtain fully mass-conserving flow (this was not done for the studies reported here).

Finally, it should be emphasized that the WOCSS approach is far more effective when there are stable stratifications present within the first few hundred meters above the surface (see, e.g., Thykier-Nielsen et al. 1990). In a deep neutral or unstable layer, the flow becomes terrain following and does not otherwise interact with the underlying terrain.

The WOCSS model has previously been applied to the Los Angeles Basin (Ludwig et al. 1991), the Vandenberg Air Force Base area of California (Thykier-Nielsen et al. 1990), and other regions. In this paper we present a systematic discussion of the model's performance in the San Francisco Bay Area (SFBA). The SFBA is a region of complex terrain (see Fig. 1), featuring a coastline aligned northwest–southeast, and a system of hills, mountains, and valleys running approximately parallel to the coast. Several gaps exists in the hills, notably the Golden Gate Gap [UTM (universal transverse Mercator) coordinates 546, 4185], the Crystal Springs Gap, (555, 4150), the Carquinez Strait (569, 4214), and the Altamont Pass (620, 4175). Under certain synoptic conditions, winds are strongly channeled through these gaps. In addition, the SFBA is generally under the influence of an elevated inversion during the warmer months of the year. Under appropriate stability conditions, the inversion can increase the channeling of flow through the gaps and down the valleys.

The SFBA is a heavily populated region replete with heavy- and high-technology industries, all of which can generate toxic releases into the air. It is obviously important to have the capability to rapidly generate accurate, high-resolution wind data for the area. It is the

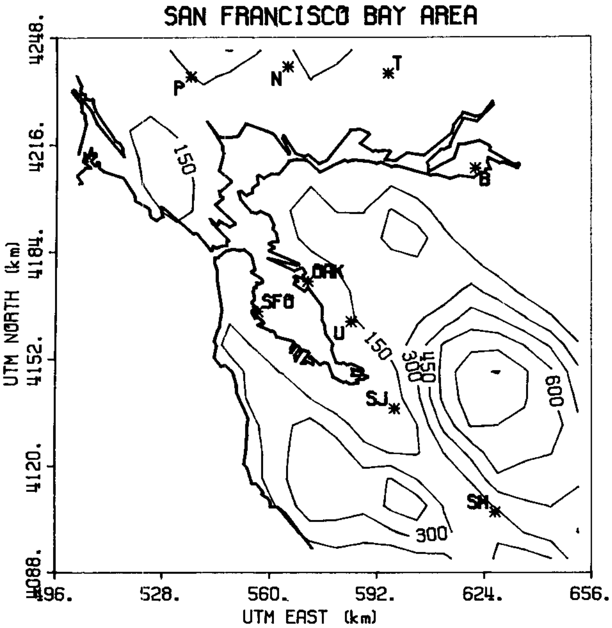

FIG. 1. The San Francisco Bay Area. Heavy line is shoreline; light lines are terrain contours (m). Also marked are sites at which data were usually available for this study: Bethel Island (B), Napa (N), Oakland (OAK), Petaluma (P), San Francisco airport (SFO), San Jose (SJ), San Martin (SM), Travis Air Force Base (T), and Union City (U).

purpose of this paper to examine and demonstrate the utility of the WOCSS code for this purpose.

Specifically, we first show results for two days that typify the northwesterly flow regime experienced in the area during the warmer months. We also examine the accuracy of wind output as a function of the amount of data input. The WOCSS code has many capabilities that can be switched on or off by the user. One is the ability to input the topography of an elevated inversion. This topography serves to configure the model's flow surfaces, which are otherwise computed internally in the manner discussed above. Below, we show wind output in two cases, one using the normal configuration of WOCSS, the other using input inversion data. Finally, as an example of the code's capability at the time of a specific event, we show results for the day of the Oakland hills firestorm, 20 October 1991.

2. Outline of case studies and model configuration

There are several synoptic situations that characterize the flow in the SFBA, the most important being the case of northwesterly (NW) flow that prevails during the summer and fall seasons. The NW flow is in response to the offshore Pacific high, together with a thermal trough located inland. The onshore component is enhanced during the day by the sea breeze and is correspondingly weakened at night (with flow reversal sometimes noted). Other flow patterns are noted in the SFBA. For example, flow with a southerly component occurs, but generally in association with the approach of fronts in winter. These are therefore of less concern since the stronger winds that often accompany these systems, together with the absence of the inversion, are conducive to the rapid dispersal of toxic spills. Occasionally a northeasterly flow develops. This was the case on the day of the firestorm and is discussed further below.

We have selected two days that typify the NW flow case. In the first case (18 November 1988; termed the *strong NW case*), a strong high pressure system was established offshore following the passage of a cold front. No inversion was present at the time, and the atmosphere over Oakland was neutrally stable. The second case (7 October 1987; termed the *weak NW case*), was characterized by a weaker pressure gradient and lighter winds. This case is more typical of summer and fall patterns in the area since an elevated inversion was present.

For both cases, surface wind observations are available hourly from eight sites (see Fig. 1). In addition, twice-daily wind and temperature radiosonde data are available from the Oakland airport site. WOCSS will accept sounding data from more than one site, but only data from the Oakland site are routinely available in the SFBA. For the weak NW case, additional surface wind data are available from 15 sites in the SFBA (their locations are indicated below). These additional data are useful in two respects: first, they allow us to compare observed and gridded winds in regions away from the original eight sites; second, they can be included to form a denser input dataset and presumably generate more accurate wind output. This sensitivity is examined below.

As mentioned above, an elevated inversion is often present in the SFBA, especially during summer and fall. During the Marine Atmospheric Boundary Layer Experiments, West Coast (MABLES WC) field experiment in August 1978 (Lester 1980; Bridger et al. 1993), detailed observations were made of meteorological conditions in the SFBA. From radiosonde, aircraft, sodar, and tower observations, datasets of inversion topography at various times were constructed. These data can be used by WOCSS to compute the flow-following coordinate surfaces. Experiments using this approach for 9 August 1978 are discussed below. For this case, surface wind data are available hourly at 10 sites in the domain (again, their locations are indicated below), as are Oakland radiosonde data.

Finally, for a specific example of the utility of the WOCSS code, we show results for 20 October 1991, the day of the firestorm in the Oakland hills. Synoptically on this date, a surface high pressure region had moved southeastward from southern British Columbia into Idaho. The pressure gradient between this and a thermal trough located over southern California produced northerly to northeasterly surface flow over the

SFBA, with strong, dry, warm downslope winds. We show below gridded winds at two times during this day and compare with observations. For this case, Oakland radiosonde soundings are available (taken at 0400 and 1600 PST), are hourly data from up to 11 sites. Here too we have additional data from 26 sites (discussed below), which again allows for more detailed comparison and analysis.

The relevant model parameters used (unless otherwise stated) are as follows: horizontal resolution is 8 km; the domain is 160 km east–west by 160 km north–south; winds are calculated on six flow surfaces that are constrained by the thermal stratification or by the specified inversion topography. In the former case, and at the lowest elevations in the domain, these surfaces are at 0, 200, 400, 700, 1000, and 2000 m AGL. Surface winds are interpolated to 10 m AGL for output.

3. Case studies

a. NW flow cases

In Fig. 2a we show the gridded winds output from WOCSS at 1600 PST for the strong NW flow case, and in Fig. 2b we show the same but at 1600 PST for the weak NW flow case. The heavy arrows in these and following figures show observed winds (i.e., input). In the strong flow case, there is a good correspondence between gridded and nearby observed winds, as anticipated. To facilitate the comparison at each observation site in this and all other cases discussed below, an average wind was constructed from data at the four surrounding grid points[1] and compared with the observation. In the strong flow case, gridded wind speed errors were less than 1 m s^{-1} at all sites, and directions were within 6° of observed wind directions at all sites. We note little tendency for flow deflection around higher elevation and through gaps in this case. In part this is due to the prevailing wind direction being closely aligned with the northwest–southeast-oriented terrain features, but it is probably more a reflection of the near-neutral stability and relatively strong winds aloft [O(10 m s^{-1}), twice as strong as in the weak flow case]. Under these conditions, the flow is not constrained to go around terrain obstacles, and thus there is little deflection.

The weak flow case is more noticeably characterized by flow guided by terrain features. Flow is funneled down the Santa Clara Valley (to the southeast of San Jose; see Fig. 1), and we note turning of the flow through both the Altamont Pass and the Carquinez Straits. Note that there is no input data in the Altamont Pass region, and only one station in the Carquinez Straits region. At five of the seven observing stations in the domain, wind speed and direction errors (as defined above) were less than 1.1 m s^{-1} and 9°, respectively. At both Napa (UTM 563, 4237) and Petaluma (534, 4234) in the north bay, speed and direction errors were larger (as high as 2.3 m s^{-1} and 22°), but inspection of Fig. 2b shows that large wind direction changes were observed over the short distance between these two sites. Given this fact, we judge the WOCSS scheme to have performed well in analyzing winds here.

As mentioned above, the Oakland sounding at this time showed an elevated inversion, and in this case the WOCSS analysis should produce flow deflection. More distinct flow channeling through the Golden Gate Gap can be generated (Becker 1992) in several ways: by using a finer resolution, the disadvantage being that arrays are then much larger, and the analysis routine is thus more time consuming; by using the WOCSS nested grid option (as many as three nested grids are allowed); or by reducing the domain size and resolution, thus keeping array size and run time fixed. For the one case examined involving the Golden Gate Gap, this last option proved most successful, but there may well be instances where other options prove more useful.

Data at 15 additional sites are available for the weak NW flow case. Figure 2c shows the WOCSS analysis when surface wind data from all 23 sites are input (heavy arrows showing observed winds also mark the additional 15 sites). A comparison of Figs. 2b and 2c shows the main effects of the added stations to be as follows: flow is accelerated and turned northeastward through the north bay due to adding the Travis Air Force Base observation (UTM 594, 4235); flow stagnation is shown upstream of the east bay hills due to adding the Richmond (557, 4200) and Walnut Creek (581, 4196) observations; flow is accelerated through the Altamont Pass region [Pleasanton (596, 4173) and Livermore (609, 4171)]; and large changes are seen in the southeast corner of the domain. San Martin (625, 4104) reported winds from 324° at the time, whereas nearby at Gilroy (630, 4095) winds were reported from 176°. The flow in this region is often influenced by inflow from the Monterey Bay region to the south, which produces a convergence zone that cannot be reproduced by a diagnostic model unless the input data are adequate to resolve its presence.

As expected, the quality of the wind analysis can be improved upon with the addition of input data. For a given region, there are likely to be key areas in which this is especially crucial. For the SFBA, for example, the flow stagnation in the east bay hills was not analyzed properly using input from the original eight stations. In turn, the analysis from WOCSS can be helpful in identifying sites where new observing platforms could be usefully located.

b. Incorporation of inversion topography

Normally, the flow-following coordinate surfaces are computed internally by WOCSS using temperature

[1] The average analyzed wind was constructed using a inverse distance–squared weighting.

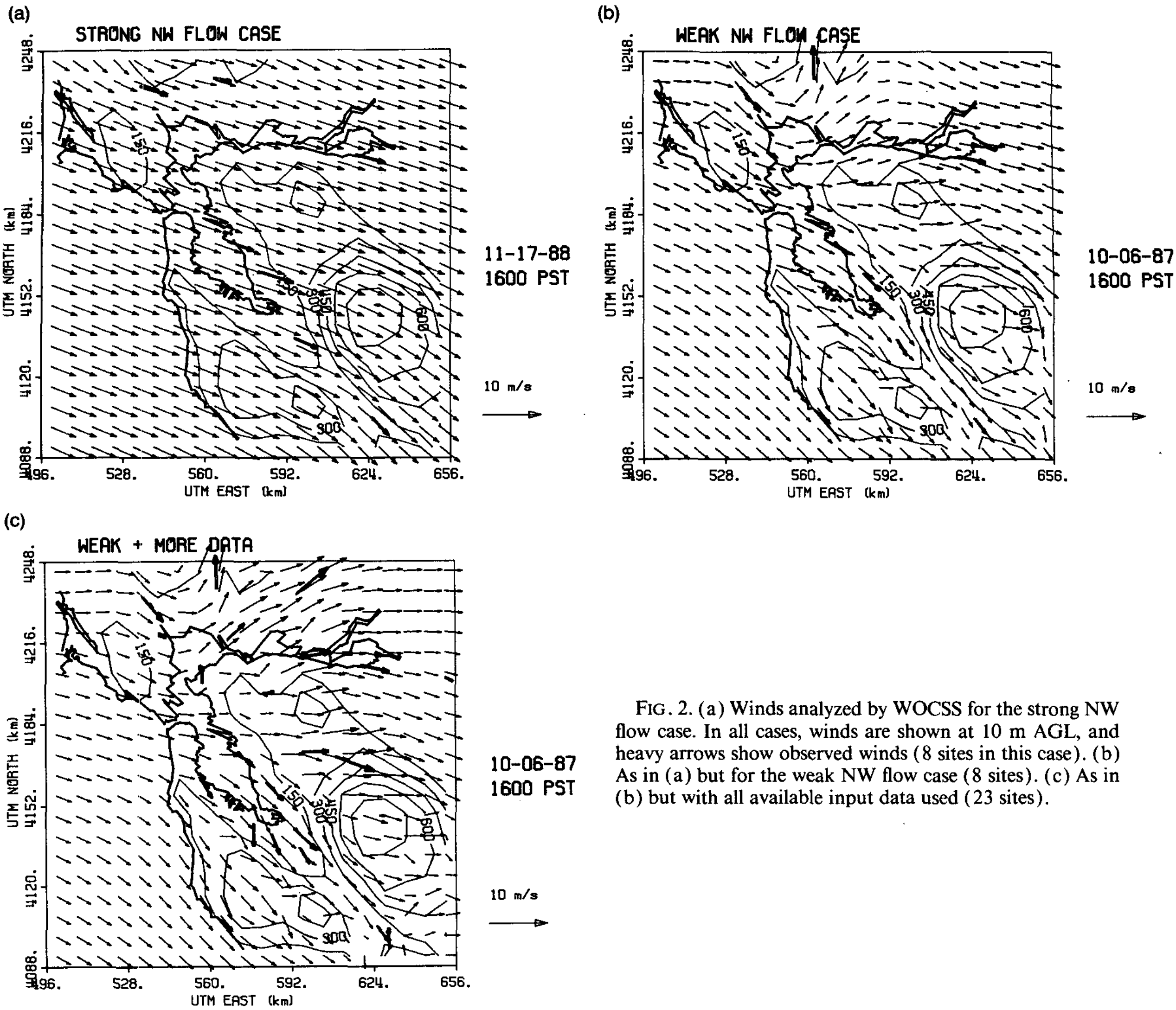

FIG. 2. (a) Winds analyzed by WOCSS for the strong NW flow case. In all cases, winds are shown at 10 m AGL, and heavy arrows show observed winds (8 sites in this case). (b) As in (a) but for the weak NW flow case (8 sites). (c) As in (b) but with all available input data used (23 sites).

sounding(s) and terrain data. In the SFBA, however, there is only one radiosonde sounding available routinely. As mentioned in the introduction, the WOCSS code allows the user to directly specify the shapes of the coordinate surfaces. Given the sparsity of upper-air data in the SFBA, it was decided to test whether WOCSS could produce more accurate surface wind analyses with this option enabled. Specifically, the WOCSS code was modified so that the elevation and shape of the highest flow surface was set equal to the elevation of the base of the inversion (recall that an elevated inversion is a ubiquitous feature of the SFBA climatology during warmer months).

As mentioned above, datasets of inversion topography are available for several days during the MABLES experiment. Using radiosonde, aircraft, sodar, and tower observations, topographic maps of the inversion base during this period were constructed. The data were digitized and input to WOCSS. In areas where no original data were available (e.g., the eastern part of the domain shown in Fig. 1), inversion topography heights were obtained by interpolation and extrapolation. In this section we analyze winds at 1600 PST 9 August 1978. Synoptic conditions during 8–10 August were fairly steady, with flow dominated by an upper-level anticyclone offshore and a thermal trough inland. Inversion base heights were near normal in the SFBA (Bridger et al. 1993), and a NW flow prevailed. The topography of the inversion on this date is typical of afternoon situations, with base elevations ranging from O(100 m ASL) over the San Francisco Bay itself, to O(300 m ASL) at the foothills, and higher over the surrounding hills. The inversion topography is very similar to that shown in Lester [(1985), Fig. 3; see also Fig. 11a in Russel and Uthe (1978)].

Figure 3a shows winds analyzed by WOCSS in the standard way with all flow surfaces internally computed (the *normal case*). In the SFBA, therefore, the upper-

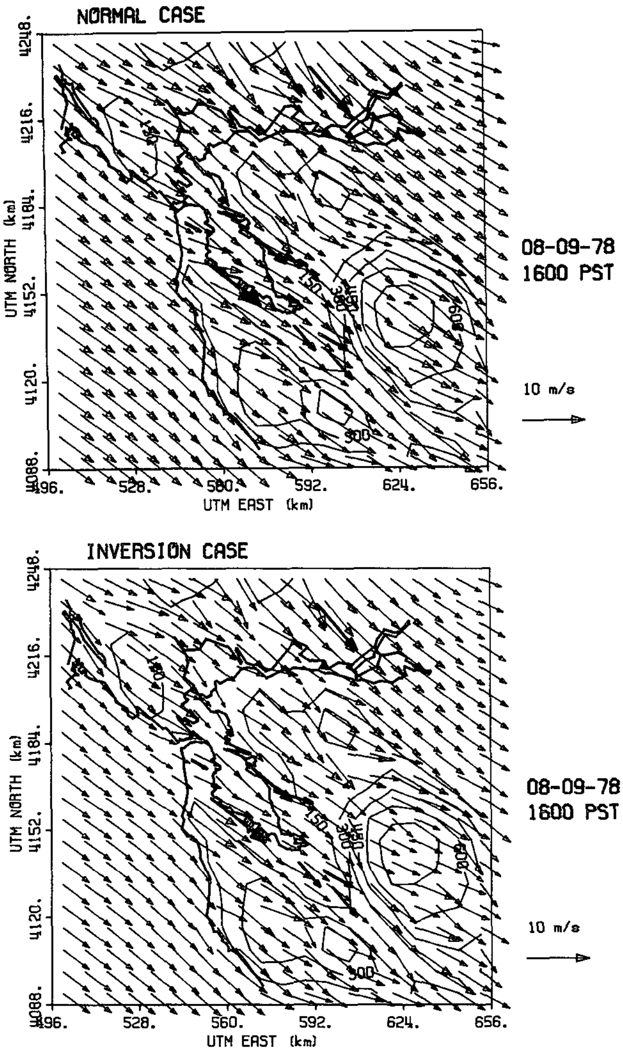

FIG. 3. Winds analyzed by WOCSS for (a) the normal case (inversion information not included; 10 sites) and (b) the inversion case (inversion information explicitly included).

flow surfaces are computed using only the Oakland sounding. Figure 3b shows winds analyzed when the inversion topography was specified (*inversion case*). The parameters input to WOCSS in the normal case were adjusted so that the average depth of the boundary layer (defined here as the distance between the uppermost flow surface and the terrain) was the same as in the inversion case (under normal conditions, an average boundary layer thickness value must be input).

The overall character of the flow in each analysis is quite similar. Analyzed winds are $O(1\text{–}2\ \mathrm{m\ s^{-1}})$ stronger in the normal case over much of the domain. Largest wind speed reductions in the inversion case occur over the highest terrain [e.g., $O(5\ \mathrm{m\ s^{-1}})$ reduction near UTM 625, 4140]. Wind directions are also modified, typically by $O(20°)$ over the highest regions. That the largest wind changes are noted over the higher elevations is in keeping with our expectation that an elevated inversion layer should serve to deflect flow around higher terrain obstacles and provides some confidence that this feature of the WOCSS scheme is operating in the desired manner.

It is not clear which of the two cases best describes the surface winds that existed across the entire domain at the time in question. As noted above, largest wind changes were found over higher terrain, areas in which surface observations were not available to validate model results. Conversely, the two analyses are most similar in the middle of the domain, where most wind input data were available. Upper-air data used to configure the flow surfaces were available only at the Oakland site, and the inversion topography dataset is based on data gathered primarily at lower elevations of the SFBA. Thus, our confidence in the results is highest for locations in the center of the domain. A closer inspection of analyzed winds at grid points surrounding the eight observing sites shows that explicit incorporation of inversion data degraded results at six of the sites [primarily with wind speeds reduced $O(1\ \mathrm{m\ s^{-1}})$].

In applications such as generating winds for input to dispersion models, accurate wind speeds and directions are desired. That being the case, we can say that explicit inclusion of inversion base topography has not demonstrably improved the analysis here. However, we have examined only one case, and it is possible that different results could be obtained in other cases and with other combinations of input parameters. The WOCSS model was designed to make maximum use of limited data. It is possible that the modifications made in order to incorporate inversion topography did not make optimum use of the added information. This problem will need more attention if the model is to be used in this manner.

c. *Firestorm case of 20 October 1991*

The Oakland foothills firestorm began (at UTM 568, 4189 approximately) in earnest late in the morning of 20 October 1991 and continued to burn into the evening hours. For this case, data are available hourly at up to 11 sites (data are missing at some sites and some hours). In addition, we have data gathered at 26 towers operated by the Bay Area Air Quality Management District (BAAQMD). The tower dataset consists of hourly averaged surface wind speeds and directions, as well as temperatures and pressures. The additional data again give us the opportunity to verify gridded output in areas away from the original sites, and in addition could be input to WOCSS with the aim of generating more accurate analyses.

The radiosonde soundings at Oakland were taken at 0400 and 1600 PST, so we first show analyses at these times. Figures 4a and 4b show gridded and observed winds at 0400 PST (five observations available) and 1600 PST (10 observations), respectively. The

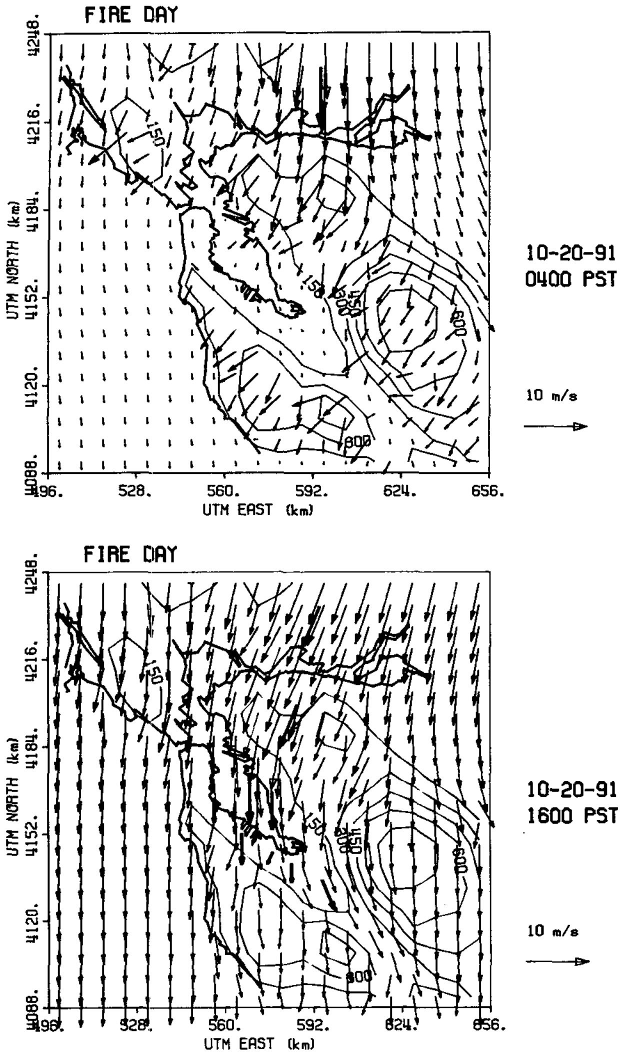

FIG. 4. Winds analyzed by WOCSS for (a) 0400 PST 10 October 1991 (5 sites) and (b) 1600 PST (10 sites).

Oakland sounding (not shown) indicates winds of 25 m s^{-1} at around 1500 m at 0400 PST and a strong ground-based inversion present at the time. Thus, strong, gusty winds were reported at higher elevations of the SFBA, with weaker winds in the valleys. The WOCSS analysis reproduces this character quite well (Fig. 4a). Gridded winds near observing sites were generally within 0.5 m s^{-1} and 10° of observed wind speeds and direction. An exception was at Travis Air Force Base. There, observed winds were from 360° at 9.4 m s^{-1}, whereas the average analyzed winds were from 4° at 7.5 m s^{-1}.

During the morning hours the inversion was destroyed, allowing stronger winds to penetrate to the surface. The WOCSS analysis for 1600 PST (Fig. 4b) shows strong flow from the north-northeast at most grid points, with channeling of the flow down the Santa Clara Valley. Comparing gridded and observed winds at the observing sites, we find that gridded wind directions were within 12° of observed wind directions, and speeds were generally within 1 m s^{-1} of observations. An exception was Palo Alto (UTM 576, 4145), which reported winds from 23° at 2 m s^{-1}. Analyzed winds at the four surrounding grid points were from 355° at 3.7 m s^{-1}. The discrepancy is undoubtedly due to the proximity of other stations reporting winds that were stronger and from more northerly directions (see Fig. 4b).

At many locations stronger winds had been reported earlier in the afternoon, so in Fig. 5a we show the gridded winds output from WOCSS for 1400 PST. For this analysis we used input data from some of the tower sites mentioned above. Specifically, data were used from the 15 sites with 10-m towers (towers at other sites are higher). Inspection of all available data suggests that conditions were quasi-steady during the early afternoon hours, so we judge the 1400 PST tower data to be representative of conditions in the SFBA at that time. The overall character of the flow at 1400 PST is quite similar to that at 1600 PST, but some differences are noted: the addition of input surface wind data in the northwestern corner of the domain produces a stronger northeasterly component in the gridded winds; the channeling of flow down the Santa Clara Valley is more evident.

Finally, in Fig. 5b we show contoured wind speeds from the WOCSS analysis at 1400 PST using input data from all 26 sites. Figure 5c shows contoured wind speeds from the WOCSS analysis for this time using input data from only the original 11 sites. Both analyses suggest that strong winds would have been expected in the same parts of the east bay at that time, but the sensitivity to the quantity of input data is apparent.

4. Conclusions

The WOCSS model has proven quite easy to use, and does not require large computing resources for its operation. All the results reported here were obtained with a 386 PC. A typical run (including graphics) is completed in $O(15\text{ s})$.

The major conclusion to be drawn is that reasonable wind analyses can be performed with this type of diagnostic model in regions of complex terrain, provided there are sufficient observations to define the key features of the flow. As is always true with diagnostic models, results are improved with more input wind data. In particular, the model needs input that can be used to diagnose flow features such as convergence zones, the bifurcation of flow (e.g., between the north and south San Francisco Bay areas), and higher speeds over peaks and ridges.

Although the addition of more surface wind observations did improve the treatment of the items listed above for the cases studied here, the changes were not always dramatic. This is encouraging because it suggests

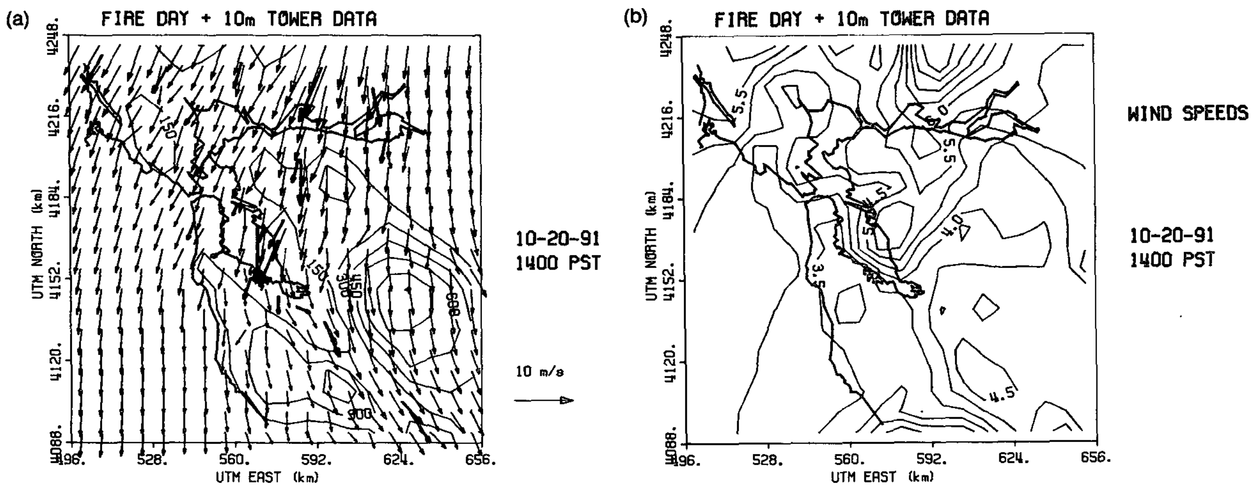

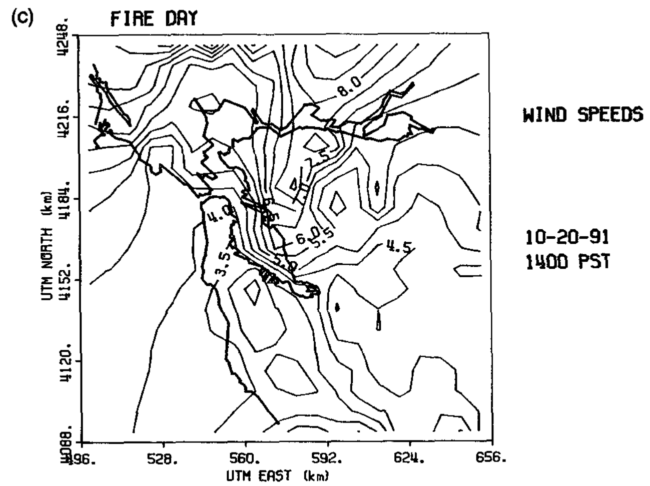

FIG. 5. (a) As Fig. 4a but at 1400 PST and with additional input data used (26 sites). (b) Contoured wind speeds (m s^{-1}) from the WOCSS analysis at 1400 PST on 10 October 1991 using input data from all 26 sites. (c) As in (b) but from the WOCSS analysis using input data from the original 11 sites.

that it is possible to specify winds in complex terrain in real time with a rather small network of stations, especially if those stations are carefully placed.

One of the more encouraging findings of this study was that detailed specification of inversion topography (as a means of specifying the topography of the upper flow surface in the model) did not improve the resulting wind estimates. This suggests that as few as one or two soundings are sufficient to specify the configuration of the flow surfaces.

Based on these case studies [and those reported in Ludwig et al. (1991)], we believe that this modeling approach is quite suitable for addressing a number of practical problems such as anemometer network design, aviation nowcasting, and teaching students about local flows and the effects of inversions on flow in complex terrain. Furthermore, it is apparent that the kinds of analyses presented here could be performed with inputs from some of the newer instruments (e.g., Doppler acoustic sounders, profilers). All these instruments provide continuous, real-time measurements that could be analyzed in real time. Toward that end, the model has recently been modified to read and decode current data files accessible by phone, perform the analyses, and display a current wind field using a PC (Becker and Sinton 1993).

Acknowledgments. The inversion topography datasets were originally synthesized from all available MABLES data by Ned Erickson and were later digitized and interpolated to a grid by Bryan Logie. The data for the Oakland firestorm date were provided by Dick Duker for the Bay Area Air Quality Management District. The assistance of these individuals is gratefully acknowledged.

REFERENCES

Anthes, R. A., and T. T. Warner, 1978: Development of hydrostatic models suitable for air pollution and other meso-meteorological studies. *Mon. Wea. Rev.*, **106**, 1045–1078.

Becker, A. J., 1992: Implementation of a mesoscale boundary layer wind model in the San Francisco Bay Area. M.S. thesis, Department of Meteorology, San Jose State University, 167 pp.

——, and D. M. Sinton, 1993: Users' guide for the Real-time Mesoscale Analysis and Display System (RMADS). COMET project final report, Department of Meteorology, San Jose State University, 44 pp.

Bridger, A. F. C., W. C. Brick, and P. F. Lester, 1993: The structure of the marine inversion layer off the central California coast: Mesoscale conditions. *Mon. Wea. Rev.,* **121,** 335–351.

Lester, P. F., 1980: Marine atmospheric boundary layer experiments, West Coast (MABLES WC). Preprints, *Second Conf. on Coastal Meteorology,* Los Angeles, CA, Amer. Meteor. Soc., 247–250.

——, 1985: Studies of the marine inversion over the San Francisco Bay Area—A summary of the work of Albert Miller, 1961–1978. *Bull. Amer. Meteor. Soc.,* **66,** 1396–1402.

Ludwig, F. L., and R. M. Endlich, 1988: Users' guide for the Winds on Critical Streamline Surfaces (WOCSS) code. Delivery Order 680 under U.S. Army Atmospheric Science Laboratory Contract DAAL03-86-D-0001, 42 pp.

——, J. M. Livingston, and R. M. Endlich, 1991: Use of mass conservation and critical dividing streamline concepts for efficient objective analysis of winds in complex terrain. *J. Appl. Meteor.,* **30,** 1490–1499.

Mass, C. F., and D. P. Dempsey, 1985: A one level mesoscale model for diagnosing surface winds in mountainous and coastal regions. *Mon. Wea. Rev.,* **113,** 1211–1227.

McNider, R. T., K. E. Johnson, and R. W. Arritt, 1984: Transferability of critical dividing streamline models to larger scale terrain. *Fourth Joint Conf. on Applications of Air Pollution Meteorology,* Portland, OR, Amer. Meteor. Soc., J25–J27.

Pielke, R. A., 1984: *Mesoscale Meteorological Modeling.* Academic Press, 612 pp.

Russel, P. B., and E. E. Uthe, 1978: Regional patterns of mixing depth and stability: SODAR network measurements for input to air quality measurements. *Bull. Amer. Meteor. Soc.,* **59,** 1275–1287.

Thykier-Nielsen, S., T. Mikkelsen, R. Kamada, and S. A. Drake, 1990: Wind flow model study for complex terrain. *Ninth Symp. on Turbulence and Diffusion,* Risø, Roskilde, Denmark, Amer. Meteor. Soc., 421–424.